Ionic Permeability Characteristics of the *N*-methyl-D-aspartate Receptor Channel

MASOUD M. ZAREI and JOHN A. DANI

From the Division of Neuroscience, Baylor College of Medicine, Houston, Texas 77030-3498

ABSTRACT *N*-methyl-D-aspartate (NMDA) receptor channels in cultured CA1 hippocampal neurons were studied using patch-clamp techniques. The purpose of the research was to determine the occupancy of the channel by permeant cations and to determine the influence of charged residues in or near the pore. The concentration dependence of permeability ratios, the mole-fraction dependence of permeability ratios, the concentration dependence of the single-channel conductance, and a single-channel analysis of Mg^{2+} block all independently indicated that the NMDA receptor behaves as a singly-occupied channel. More precisely, there is one permeant cation at a time occupying the site or sites that are in the narrow region of the pore directly in the permeation pathway. Permeability-ratio measurements in mixtures of monovalent and divalent cations indicated that local charges in or near the pore do not produce a large local surface potential in physiologic solutions. In low ionic strength solutions, a local negative surface potential does influence the ionic environment near the pore, but in normal physiologic solutions the surface potential appears too small to significantly influence ion permeation. The results indicate that the mechanism for the high Ca^{2+} conductance of the NMDA receptor channel is not the same as for the voltage-dependent Ca^{2+} channel (VDCC). The VDCC has two high affinity, interacting binding sites that provide high Ca^{2+} selectivity and conductance. The binding site of the NMDA receptor is of lower affinity. Therefore, the selectivity for Ca^{2+} is not as high, but the lower affinity of binding provides a faster off rate so that interacting sites are not required for high conductance.

INTRODUCTION

The *N*-methyl-D-aspartate (NMDA) subtype of glutamate receptors is a ligand-gated cation-selective ion channel that is highly permeable to Ca^{2+} and is blocked by Mg^{2+} in a voltage-dependent manner (Nowak, Bregestovski, Ascher, Herbet, and Prochiantz, 1984; Mayer, Westbrook, and Guthrie, 1984; MacDermott, Mayer, Westbrook, Smith and Barker, 1986; Jahr and Stevens, 1987). These ion permeation properties underlie the role of the NMDA receptor in the induction of long-term potentiation at several excitatory pathways in the central nervous system (review by Bliss and Collingridge, 1993). Although these properties of ion movement through the NMDA

Address correspondences and reprint requests to John A. Dani, Division of Neuroscience, Baylor College of Medicine, One Baylor Plaza, Houston, TX 77030-3498.

J. GEN. PHYSIOL. © The Rockefeller University Press · 0022-1295/94/02/0231/18 $2.00
Volume 103 February 1994 231–248

receptor channel have been clearly demonstrated, the mechanisms that underlie these properties are controversial.

An important determinant of the permeability characteristics of an ion channel is the number of ions that occupy the narrow region of the pore. This region contains the ion binding sites that are directly in the permeation pathway, and therefore, these sites must be encountered by every ion that passes through the pore. Several pieces of evidence suggest that there may be multiple occupancy of the NMDA receptor pore. When an open-channel blocker apparently senses more than 100% of the voltage drop across the membrane, that indicates that the blocker is coupled to other ions in the permeation pathway (i.e., multiple occupancy). In several cases, it has been reported that blockers of the NMDA receptor may sense up to 100% of the field (Ascher and Nowak, 1988; Mayer, Westbrook, and Vyklicky, 1988; but see Jahr and Stevens, 1990). In addition, when a blocker was applied first to the outside of the channel then the inside, the proportion of the field sensed from the two sides added up to greater than 100%, suggesting that the blocking ion is coupled to the movement of permeant ions (Ascher and Nowak, 1988; Johnson and Ascher, 1990). Other evidence indicates that the open channel blockers, MK-801 and Mg^{2+}, interact with each other or with Ca^{2+} (Mayer and Westbrook, 1987; Ascher and Nowak, 1988; Huettner and Bean, 1988). Although much of the work suggests there may be competition among these ions for a single site, at very low salt concentrations the interaction between MK-801 and Mg^{2+} does not seem strictly competitive (Reynolds and Miller, 1988). In low concentrations of salt, it also was found that reversal potential measurements could not be described by a simple single occupancy permeation model (Mayer and Westbrook, 1987).

In many of the cases described above, the results also could be explained by single occupancy of the pore if, in addition, there are local negative charges that influence ion permeation. Local net negative charge in or near the pore can be thought of as producing a local "surface potential." There is controversy about the existence or strength of a local surface potential. It was found that a small local surface potential could explain the increased permeability ratio of Ca^{2+} to Na^+ (P_{Ca}/P_{Na}) in low ionic strength solutions. Although multiple occupancy of the pore could produce the result, an equally good explanation was that a small negative surface potential present in low ionic strength solutions elevates the local concentration of Ca^{2+} in relation to that of Na^+ and produces an apparent increase in the permeability ratio (P_{Ca}/P_{Na}; Mayer and Westbrook, 1987; Iino, Ozawa, and Tsuzuki, 1990). On the other hand, a much larger negative local surface potential present even in high ionic strength solutions was proposed to explain single-channel current-voltage relations in mixtures of Ca^{2+} and Na^+ (Ascher and Nowak, 1988).

The purpose of this study was to resolve these controversies by determining whether the NMDA receptor channel is multiply occupied and by determining the influence of a local surface potential. The concentration dependence of the permeability ratio of two permeant cations, the mole-fraction dependence of the permeability ratio, the shape of the concentration dependence of the single-channel conductance, and a burst analysis of Mg^{2+} block all separately indicate that the NMDA receptor behaves as a single-occupancy channel. The influence of local charges in or near the channel was investigated by measuring permeability ratios in different ionic

strength mixtures of monovalent and divalent cations. Measurements in a wide range of solutions indicate that a low density of net negative charges influence ion permeation through the NMDA receptor. Only in low ionic strength solutions, not in physiologic solutions, is the permeability ratio of divalent to monovalent cations affected by a local surface potential. Some of this work was previously reported at a scientific meeting (Zarei and Dani, 1992).

MATERIALS AND METHODS

Cell Culture

Hippocampal neurons were cultured using standard techniques (adapted from Huettner and Baughman, 1986; Amador and Dani, 1991*a*). In short, two Sprague-Dawley rats (postnatal day 1–2) were used for each preparation. The brain was removed and was kept in Earl's balanced salt solution (EBSS) throughout the dissection. The CA1 region was dissected from the hippocampus, and the isolated CA1 tissue was then transferred into an enzyme solution containing 10 ml of EBSS and 200 U of papain for ~30 min (Worthington Biochemical Corp., Freehold, NJ). The tissue was washed several times with complete media that also contained 2.5 mg/ml trypsin inhibitor and bovine serum albumin (Sigma Chemical Co., St. Louis, MO). Then, the tissue was gently triturated with the same solution to dissociate the cells. Complete media was composed of Minimum Essential Medium (GIBCO Laboratories, Grand Island, NY), 292 μg/ml glutamine, 5% heat-inactivated fetal bovine serum (Hyclone Labs, Logan, UT), 50 U/ml penicillin, 50 μg/ml streptomycin, 20 mM glucose, and 1 μl/ml serum extender (Collaborative Research, Inc., Bedford, MA). The cells were plated onto coverslips that had been coated with collagen and poly-D-lysine and exposed to ultraviolet light for 30 min. After 3 d, the cells were treated for 2 d with 5 μM cytosine arabinofuranoside. The cells were maintained in complete media in an incubator at 37°C, 5% CO_2. Media was changed every 3 d, and the cells were used between 6 to 9 d after plating. Although the cells were healthy for much longer, we used them early and for a short period of time so that the cells did not have extremely long processes.

Patch-Clamp Techniques

Whole-cell and single-channel NMDA receptor currents were measured using standard patch-clamp techniques (Hamill, Marty, Neher, Sakmann, and Sigworth, 1981; Dani, 1989). Electrodes were pulled with a two-stage electrode puller (PP-83; Narishige USA, Inc., Greenvale, NY) using Garner Glass 7052 and were coated with Sylgard silicon elastomer (Dow Corning Corp., Midland, MI). The tips of the electrodes were polished immediately before they were used with a microforge (MF-83; Narishige USA, Inc.). Their resistances were between 2 to 5 MΩ in standard solutions.

Currents were amplified and filtered using an Axopatch 1B voltage clamp with a 4-pole Bessel filter (Axon Instruments, Foster City, CA). Currents were digitally sampled with a 12-bit analog-to-digital converter (TL-1; Axon Instruments). The computer system delivered the holding potentials through a 12-bit digital-to-analog output. Whole-cell currents were sampled every 20 ms, and the currents were measured 2 s after the application of agonist. Single-channel currents were sampled every 0.1 ms. Various filter settings were used.

Complete solution changes were achieved by using large inflow pipettes. These inflow pipettes (KG-33; Garner Glass, Claremont, CA) had wide openings (380-μm inner diam) and narrow walls and were arranged in a row and glued together (see Amador and Dani, 1991*b*; Vernino, Amador, Luetje, Patrick, and Dani, 1992). These pipettes were mounted on a hydraulic manipulator that allowed rapid solution changes. Fast solution changes, however,

were not critical for measuring steady state currents after the application of agonist. For whole-cell experiments, measurements in test solutions were always bracketed by measurements in a control solution. Control solutions contained the same composition as the test solutions except the main charge carrying ion was Cs^+. In all experiments, the liquid junction potentials were measured, and the holding potentials were corrected before plotting the data. Depending on the solutions, the liquid junction potentials varied from 0 to 3 mV. All the experiments were conducted at room temperature, 23°C.

Solutions

A wide range of electrolyte solutions were used to study whole cells and outside-out membrane patches. The osmolalities of all the solutions were measured with a vapor pressure osmometer (Wescor, Inc., Logan, UT) and adjusted to appropriate values by adding sucrose. The pH of the solutions was adjusted to 7.4 using the hydroxide of the main cation. Unless stated otherwise, the bath was (mM) 150 NaCl, 3 KCl, 2 $CaCl_2$, 10 HEPES, 10 glucose, 50 μM picrotoxin, 1 μM strychnine, 0.5 μM tetrodotoxin and 200 μM DIDS. The external solutions in the inflow pipettes had the same channel blockers (without DIDS) as the bath solution (ultra pure salts, Johnson Matthey, Inc., Wayne, PA). On the day of the experiment, 20 μM NMDA (Cambridge Research Biochemical, Inc., Wilmington, DE) and 10 μM glycine were added to the external solutions for whole-cell recordings and 1–3 μM NMDA and glycine were added for single-channel recordings.

The cations used in the permeability-ratio experiments were dimethylammonium (DMA^+) and Cs^+. These cations were chosen because their permeabilities were different enough to produce easily measured shifts in the reversal potentials. The external solution was (mM) 500 or 150 DMA^+, 10 HEPES plus blockers. The internal solution was (mM) 500 or 150 CsCl, 0.1 $CaCl_2$, 10 HEPES, 5 Na-ATP, 5 EGTA. The solutions for experiments at a monovalent cation concentration of 50 or 10 mM were obtained by diluting the 150 mM solutions and, then, adjusting the osmolalities to 0.3 osMo with sucrose. The HEPES concentrations were adjusted to 5 mM, and the concentration of blockers were adjusted to the concentrations used in the original bath solution. Unless stated otherwise these external solutions were nominally free from divalent cations.

The same cations that were used for the permeability-ratio experiments also were used in the mole-fraction experiments. Two external solutions nominally free from divalent cations were used. One solution contained (mM) 150 DMA^+, 10 HEPES plus blockers, and the second solution contained 150 CsCl, 10 HEPES plus blockers. Appropriate ratios of these two solutions were mixed to obtain the following mole fractions of DMA^+: 1 (150 mM DMA^+), ⅞, ¾, ½, ¼, ⅛, 1/16, 0 (150 mM CsCl). The internal solution was always (mM) 150 CsCl, 0.1 Ca, 10 HEPES, 5 Na-ATP, 5 EGTA.

Ammonium was used as the permeant ion to measure the concentration dependence of the single-channel conductance. Ammonium was chosen because it has a high conductivity through the NMDA receptor channel, which produces large single-channel currents that could be accurately measured even in low salt concentrations. Because low concentrations of divalent cations can influence the single-channel currents carried by monovalent cations (Dani and Eisenman, 1987; Jahr and Stevens, 1990), the external solution bathing the patch was nominally free from divalent cations: 150 or 400 mM NH_4Cl, 20 HEPES plus blockers. The internal solution contained (mM) 135 or 385 NH_4Cl, 15 EGTA, 20 HEPES. When the pH of these solutions was adjusted with NH_4OH, the final concentrations of NH_4^+ became 150 and 400 mM. The solutions used for measurements in 50, 20, and 7 mM NH_4Cl were prepared by diluting the 150 mM solutions as explained in the permeability-ratio experiments. In addition, at 7 mM NH_4Cl we also added 0.5 mM EGTA and EDTA to the external solution to be certain that divalent cations were not influencing the results.

Permeability ratios of divalent cations to monovalent cations were measured using solutions that were similar to those described above, but 0.5 mM Ca^{2+} was added to the external solution of 150 mM DMA^+. That solution was diluted to 50 and 10 mM as explained above, and the internal solutions were the same as the internal CsCl solutions described above. Permeability ratios were also measured in external mixtures of Cs^+ with Ba^{2+} or Ca^{2+}. A solution of 150 mM CsCl, 10 mM HEPES plus blockers was mixed with an identical solution that also contained either 30 mM Ba^{2+} or Ca^{2+}. By mixing appropriate ratios of these two solutions, external solutions were created that contained 150 mM CsCl, 10 HEPES plus 1.5 or 15 or 30 mM $BaCl_2$ or $CaCl_2$. The internal solution was (mM) 135 CsCl, 0.1 $CaCl_2$, 10 HEPES, 5 Na-ATP, 15 EGTA, 15 EDTA. For a second set of experiments, these solutions were diluted to 10 mM as described above and the osmolalities were adjusted to 0.3 osMol with sucrose. The bath solutions in these experiments contained 150 mM CsCl, 10 mM HEPES, 0.5 mM $CaCl_2$ plus blockers.

In all calculations and for graphs that showed theoretical lines, the activities of cations were always used. The following method was used to determine activity coefficients. The ionic strength of the solution was calculated and was used to look up the activity coefficient from tables of that electrolyte. The tables were from the CRC Handbook of Chemistry and Physics, Edition 65, 1984, and from the Journal of Physical Chemistry Reference Data, Vol. 6, 1977. To obtain the single ion activity coefficients for divalent cations we followed the convention of Butler (1968), who suggests that a divalent cation's activity coefficient is given by $\gamma_{++} = (\gamma)^2$. In the cases were calculations were made using activities, we give the activity of each cation in parenthesis after the concentration (e.g., 150 (112) mM CsCl).

Because the solution in the patch pipette was often very different from the cytoplasmic electrolyte, >8 min were allowed for the pipette electrolyte to diffuse throughout the cell. By following the shift in the reversal potential, it was found that a steady value was reached after 6 min in large cells, indicating that the internal exchange of electrolyte was sufficiently complete in <6 min with the smaller cells that were used in the experiments described in this paper.

RESULTS

Occupancy of Ion Binding Sites Directly in the Permeation Pathway of the NMDA Receptor Pore

Permeability-ratio experiments were used to determine whether the NMDA receptor channel is singly or multiply occupied by permeant cations directly in the permeation pathway. If the reversal potential of two permeant ions remains constant as a function of concentration, that is strong evidence that the channel is singly occupied (see Levitt, 1986; Dani, 1989). Reversal potentials were measured using Cs^+ as the internal permeant cation and DMA^+ as the external permeant cation. The ionic concentrations of Cs^+ and DMA^+ were changed together from 10 to 500 mM, and the reversal potentials were measured at each concentration (Fig. 1). An analysis of variance showed that the measured reversal potentials did not change significantly as a function of concentration ($P > 0.05$): the permeability ratio remained constant, $P_{Cs}/P_{DMA} = 4.8$. These results indicate that the NMDA receptor channel behaves as though there is a single cation at a time occupying the site(s) directly in the permeation pathway over the concentration range that was studied.

Mole-fraction experiments were conducted to confirm the conclusion of the permeability-ratio experiments. If the reversal potential varies monotonically as the mole fraction of two permeant cations is varied, then the result indicates that the

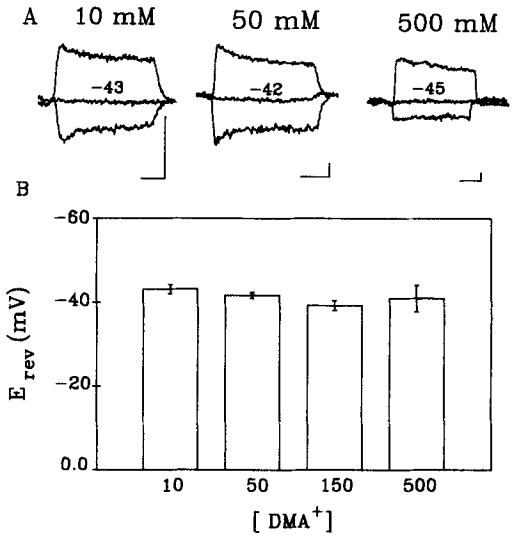

FIGURE 1. Concentration dependence of bi-ionic reversal potentials measured with DMA^+ outside and Cs^+ inside. (*A*) Whole-cell, agonist-induced currents are shown at three concentrations as labeled. Currents are shown at the following holding potentials: −30, −43, −50 at 10 mM; −30, −42, −50 at 50 mM; −38, −45, −48 at 500 mM. Although currents were measured at other holding potentials, they are not shown to simplify the figure. The three scale bars each represent 20 pA and 1 s. (*B*) The reversal potentials (n = 3, SEM) are shown as a function of concentration. The reversal potentials are not significantly different, indicating that the NMDA receptor is singly occupied.

channel is singly occupied (Neher, 1975). Reversal potentials were measured with 150 mM Cs^+ as the internal permeant cation and with different mole fractions of DMA^+/Cs^+ as the external permeant cations. When the mole fraction of the DMA^+ was changed from 0 up to 1, the reversal potential changed monotonically (Fig. 2), indicating that the NMDA receptor channel behaves as though it is singly occupied by a permeant cation directly in the permeation pathway.

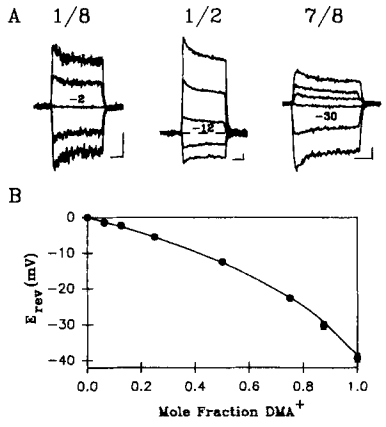

FIGURE 2. Mole-fraction dependence of reversal potentials measured with 150-mM mixtures of DMA^+ and Cs^+ outside and 150 mM Cs^+ inside. (*A*) Whole-cell, agonist-induced currents are shown at three mole fractions as labelled. The reversal potentials are given for each set of currents. Currents are shown at the following holding potentials: 8, 3, −2, −7, −12 mV for a mole fraction of ⅛; 0, −5, −10, −15, −17 for a mole fraction of ½; −23, −26, −28, −30, −36, −43 for a mole fraction of ⅞. Although currents were measured at other holding potentials, they are not shown to simplify the figure. The three scale bars each represent 25 pA and 1 s. (*B*) The reversal potentials (n = 3, SEM) are plotted versus the mole fraction of DMA^+. The line drawn through the data is based on a constant permeability ratio, P_{Cs}/P_{DMA} = 4.8. The monotonic decline in the reversal potential indicates that the NMDA receptor is singly occupied.

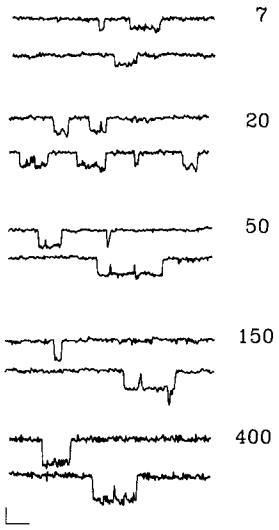

FIGURE 3. Concentration dependence in ammonium solutions of single-channel currents. Examples of single-channel currents at a holding potential of −30 mV are shown for symmetrical solutions of NH_4^+ given in mM next to each pair of records. Notice that the currents in 7 mM NH_4^+ are still quite large. The scale bars are 2 pA and 10 ms.

Concentration Dependence of the Single-Channel Conductance

The single-channel conductance of the NMDA receptor was measured in five different concentrations of NH_4^+. In these experiments, equal concentrations of NH_4^+ bathed both sides of the membrane. The concentration of NH_4^+ was changed from 7 (6.4) mM up to 400 (272) mM, and Fig. 3 shows examples of single-channel currents. In each concentration, the mean zero-voltage conductance of the NMDA receptor channel was determined (Fig. 4). Then, the experimental data were fitted

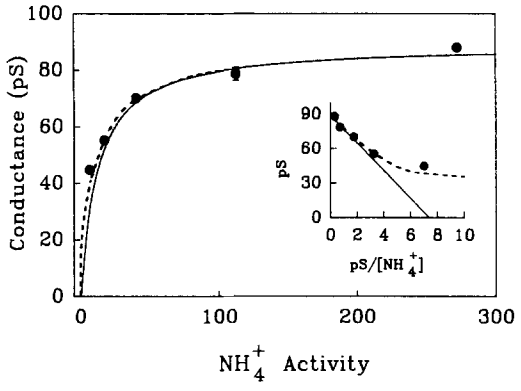

FIGURE 4. Concentration dependence of the zero-voltage single-channel conductance. The single-channel conductance is plotted versus the symmetrical activity of NH_4^+. The zero-voltage conductance was determined from the slope of the current-voltage relation through zero. Conductances determined from separate patches or from extremes in the slope used to describe the data allowed us to estimate the error, which is showed as a bar when it is greater than the symbol. The insert is an Eadie-Hofstee plot of conductance versus conductance divided by NH_4^+ activity. The solid theoretical line represents a single-site model based on Eq. 1 with a γ_{max} of 90 pS and a K_M of 12 mM. The dashed theoretical curve represents a single-site model that also includes a small negative charge density of 0.02 charges per nm^2. The negative charge produces a negative local potential that influences the concentration of NH_4^+ next to the channel only in low concentrations. The same theoretical lines are shown both in the insert and in the main graph.

using the Michaelis-Menten (*M-M*) single-site equation:

$$\gamma_0 = \frac{\gamma_{max}[NH_4]_b}{K_M + [NH_4]_b} \quad (1)$$

where γ_0 is the measured conductance, γ_{max} is the maximum conductance, K_M is the *M-M* dissociation constant for NH_4^+, and $[NH_4]_b$ is the bulk activity of NH_4^+. The conductance of a channel with multiple occupancy can reach a maximum and, then, decrease at higher concentrations of the permeant cation. The single-channel conductance of the NMDA channel, however, begins to level off at higher concentrations of NH_4^+ as expected when a single site is becoming saturated (Fig. 4). This behavior is consistent with the earlier permeability-ratio and mole-fraction experiments. However, at 7 mM NH_4^+, the conductance of the channel is higher than predicted by simple, single-site kinetics. In the inset of Fig. 4, the data are recast as an Eadie-Hofstee plot that more clearly shows the deviation at the lower concentrations. This type of deviation is often explained by assuming that the channel is multiply occupied, but that cannot be the case here. An equally good explanation for the deviation is that at very low electrolyte concentrations a local negative surface potential attracts NH_4^+ to the pore and increases the effective local concentration of the permeant cation (see Dani and Eisenman, 1987; Green and Andersen, 1991). The solid line in Fig. 4 shows the behavior of a simple, single-site description of conductance (Eq. 1). The dotted line shows that by introducing a small surface potential (described below) the single-site model more closely describes the deviation to a higher conductance that is seen in 7 (6.4) mM NH_4^+. This result lead us to investigate more thoroughly the influence of local net negative charges in or near the NMDA receptor channel.

Interactions Between the Blocking Ion, Mg^{2+}, and the Permeant Ion, Cs^+

The previous experiments showed that the NMDA receptor behaves as a single-occupancy channel for permeant monovalent cations. Here we provide evidence that the interaction between Cs^+ and the blocking ion, Mg^{2+}, is consistent with single occupancy. It is known that external Mg^{2+} blocks by entering deeply into the pore like a cork in a bottle (Mayer et al., 1984; Nowak et al., 1984). If there were multiple sites, after Mg^{2+} binds to its blocking site other ions binding to a more external site would trap Mg^{2+} in the pore, enhancing the block as is seen for the multiple sites of the Ca^{2+}-activated K^+ channel (Cecchi, Wolff, Alvarez, and Latorre, 1987; Neyton and Miller, 1988). Fig. 5 *A* shows single-channel, NMDA receptor currents in pure 50 mM Cs^+ and when 7 (2.4) μM Mg^{2+} is added to the external solution. The rapid block caused by Mg^{2+} is easily seen as flicker. When 7 μM Mg^{2+} is added to the external solution of 50 mM Cs^+, the number of openings per burst increases from 1.5 ± 0.1 to 3.3 ± 0.2 and the fraction of time a channel is open during a burst falls from 0.92 ± 0.02 to 0.74 ± 0.03 (n = four patches with 259, 415, 62, and 188 bursts per patch). This protocol was repeated in pure 200 mM Cs^+ (Fig. 5 *B*). To have the same amount of Mg^{2+} near the channel at 200 mM Cs^+, we corrected the activity of Mg^{2+} for the influence of ionic strength in the bulk solution as described in the methods and for the small difference in the surface potential, which is −1.9 mV in 50

mM CsCl and −0.5 in 200 mM CsCl (from Fig. 4). Thus, 10.5 (2.6) μM Mg^{2+} was added to the 200 mM Cs^+, and Fig. 5 *B* shows that there is less rapid block than was seen at the lower ionic strength, Fig. 5 *A*. When 10.5 μM Mg^{2+} is added to the external solution of 200 mM Cs^+, the number of openings per burst increases from 1.6 ± 0.1 to 2.5 ± 0.3 and the fraction of time a channel is open during a burst falls from 0.93 ± 0.01 to 0.84 ± 0.01 (n = three patches with 241, 483, and 95 bursts per

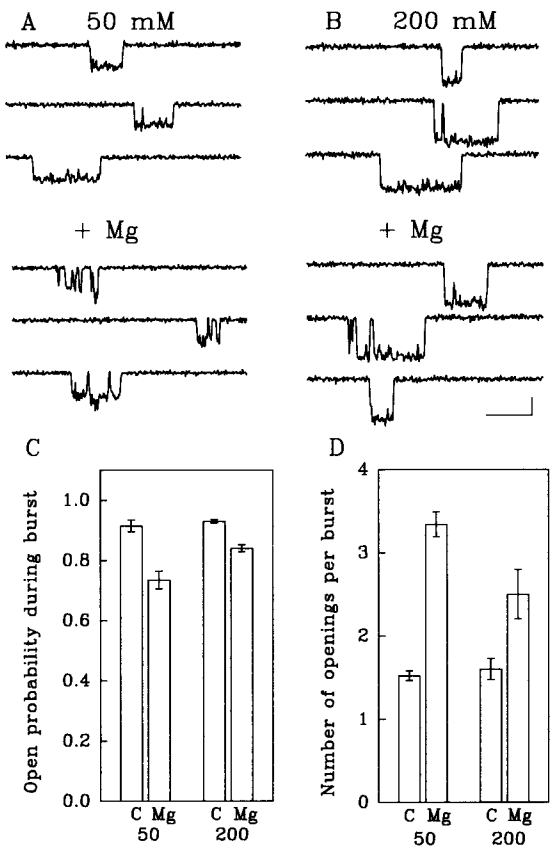

FIGURE 5. Mg^{2+} blockade of NMDA receptor single-channels in 50 and 200 mM Cs^+. The holding potential was −60 mV; the sampling rate was 10 kHz; the filtering rate was 2 kHz. The concentration of agonist was 1 μM NMDA and 1 μM glycine. (*A*) Single-channel currents are shown in 50 mM Cs^+ without (above) and with (below) 7 (2.4) μM Mg^{2+} added to the external solution. (*B*) Single-channel currents are shown in 200 mM Cs^+ without (above) and with (below) 10.5 (2.6) μM Mg^{2+} added to the external solution. The scale bars represent 2 pA and 10 ms. (*C*) The bar graph shows the probability of a channel being open during a burst in 50 or 200 mM Cs^+ with (labeled *Mg*) or without (labeled *C* for control) added Mg^{2+}. (*D*) The bar graph shows the number of openings per burst in 50 or 200 mM Cs^+ with (labeled *Mg*) or without (labeled *C*) added Mg^{2+}. Based on the closed-time distributions a critical closed time of 5 ms was used for the burst analysis. The data also were analyzed using a critical closed time of 2 ms, which gave the same results. The Mg^{2+}-free control solutions contained 1 mM EDTA. The Mann-Whitney U test indicates that there is significantly less Mg^{2+} blockade in 200 mM versus 50 mM Cs^+.

patch). The raw data and the burst analysis (Fig. 5, *C* and *D*) indicate that the block by Mg^{2+} is diminished by increasing the concentration of Cs^+. This result is not like the increased block at higher concentrations of the permeant ion that is seen with multi-site channels (Cecchi et al., 1987; Neyton and Miller, 1988). Rather, the result is consistent with a single-occupancy pore. Cs^+ competes with Mg^{2+} for occupancy of the pore; thus, as the Cs^+ concentration is elevated the Mg^{2+} block is less apparent.

Local Net Negative Charge Influences Ion Permeation

The influence of local net negative charge on the ionic environment near the channel can be studied using different ionic strength solutions. In high ionic strength solutions, the charges near the pore are screened by the electrolytes (reviews by McLaughlin, 1977; Green and Andersen, 1991). In low ionic strength solutions, however, the charges are not screened as well. Therefore, the net negative charge produces a larger potential that more strongly attracts cations toward the pore. Divalent cations are attracted more strongly than are monovalent cations, causing the ratio of divalent cations to monovalent cations to increase in lower ionic strength solutions. In that case, adding permeant divalent cations into a solution will cause a

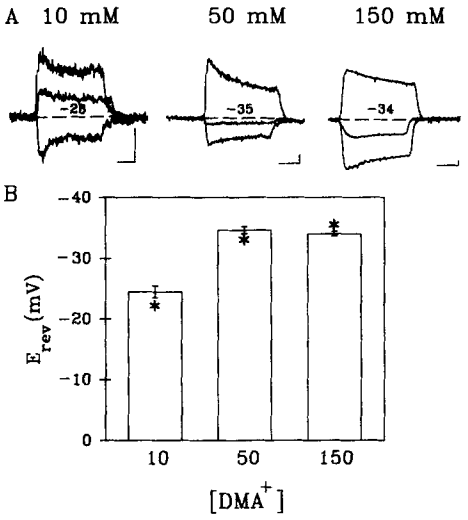

FIGURE 6. Reversal potential measurements in different ionic strength mixtures of DMA^+ and Ca^{2+}. (*A*) Agonist-induced, whole-cell currents are shown at three different concentrations of the cations. One concentration consisted of 150 mM Cs^+ inside and 150 mM DMA^+ plus 0.5 mM Ca^{2+} outside the cell (labeled 150 mM) The other currents are in solutions obtained by diluting the first solutions by 3 (labeled 50 mM) and by 15 (labeled 10 mM). The reversal potentials are given for each set of currents. Currents are shown at the following holding potentials: −13, −20, −33 mV at 10 mM; −22, −37, −42 mV at 50 mM; −24, −37, −44 at 150 mM. The scale bars represent 10 pA and 1 s. Although currents were measured at other holding potentials, they are not shown to simplify the figure. (*B*) The reversal potentials ($n \geq 3$, SEM) are shown as a function of concentration. The reversal potentials are not significantly different at the two higher concentrations, but the reversal potential is depolarized at the lowest concentration. The theoretical predictions (*) were produced by a low negative charge density near the pore (0.02 charges per nm^2).

greater positive shift in the reversal potential if the solution is of low ionic strength. We investigated the influence of the local net negative charges in or near the NMDA receptor by measuring reversal potential shifts in mixtures of monovalent and divalent cations that were of different ionic strength.

Reversal potentials were measured in solutions that had the ratio of the cations fixed while the concentrations were varied. The internal solution was pure Cs^+ and the external solution was a mixture of DMA^+ and Ca^{2+}. Fig. 6*A* shows examples of the measurements in three different concentrations of the cations. One concentration consisted of 150 mM Cs^+ inside and 150 (113) mM DMA^+ plus 0.5 (0.12) mM Ca^{2+} outside the cell. Those solutions were diluted by a factor of 3 and by a factor of 15 to obtain the other two solutions. Because the ratio of DMA^+ to Ca^{2+} in the external

bulk solution remained unchanged, the reversal potential should have remained constant unless a local surface potential altered the ratio of the cation concentrations next to the pore. The open bars in Fig. 6 *B* show that the reversal potential is the same at 150 (113) mM DMA^+ plus 0.5 (0.12) mM Ca^{2+} and 50 (40) mM DMA^+ plus 0.17 (0.057) mM Ca^{2+} but in 10 mM (9) DMA^+ plus 0.033 (0.016) mM Ca^{2+} the reversal potential is more positive. The result is consistent with a small local negative potential increasing the ratio of the Ca^{2+} concentration to that of the DMA^+ concentration next to the pore only in the low ionic strength solution.

The extended Goldman-Hodgkin-Katz (GHK) equation (Lewis, 1979; Lewis and Stevens, 1979) was used to calculate the permeability ratios, P_{Ca}/P_{DMA}, from the reversal potential (E_{rev}) measurements:

$$\frac{P_{Ca}}{P_{DMA}} = \frac{(1 + e^{FE_{rev}/RT})\left(\frac{P_{Cs}}{P_{DMA}}[Cs]_i e^{zFE_{rev}/RT} - [DMA]_b\right)}{4[Ca]_b}. \quad (2)$$

Activities were used for the calculations, with $[Ca]_b$ and $[DMA]_b$ representing the bulk activity of Ca^{2+} and DMA^+. $[Cs]_i$ represents the activity of internal Cs^+. P_{Cs}/P_{DMA} was determined in the earlier experiments shown in Fig. 1. When experimental E_{rev} values were substituted into Eq. 2, the apparent P_{Ca}/P_{DMA} was significantly increased in the 10 mM electrolyte solution. As was shown earlier (Figs. 1 and 2) and will be shown below (Fig. 7) permeability ratios are constant as activity is changed. Therefore, the apparent increase in P_{Ca}/P_{DMA} is caused by local net negative charges in or near the pore. In 10 mM DMA^+, the local charges are not effectively screened by the low ionic strength. Therefore, Ca^{2+} is concentrated at the pore more than DMA^+. Because the surface ratio of the activities, $[Ca^{2+}]_s/[DMA^+]_s$, is greater than the bulk ratio of the activities, $[Ca^{2+}]_b/[DMA^+]_b$, Ca^{2+} causes a larger shift in the reversal potential at low ionic strength. The differences between the surface activities of the cations and the bulk activities can be approximated using the Boltzmann's equation:

$$[X]_s = [X]_b e^{-zF\Psi/RT} \quad (3)$$

where $[X]_s$ and $[X]_b$ represent surface and bulk activity of ions respectively, and Ψ represents the potential created by the net negative charges in or near the NMDA pore. Ψ can be crudely approximated by using Grahame's equation (Grahame, 1947):

$$\sigma = \left(\frac{1}{G}\right)\left[\sum_{i=1}^{n} X_i(e^{-zF\Psi/RT} - 1)\right]^{1/2} \quad (4)$$

where σ is the charge density in electronic charges per nm^2, G is a constant with a value of 2.7 $(nm^2/charge)\ (mol/liter)^{1/2}$, X_i is the activity of the ith ion species in the bulk solution, and Ψ is the potential created by the charge. This approach only roughly approximates the likely dynamic situation of discreet dipoles and charged amino acids distributed in or near the NMDA receptor pore (see McLaughlin, 1977; Dani, 1986). However, the underlying principles are similar, and thus the approach provides a basis for analysis and discussion. The analysis indicates there is a low negative charge density of 0.02 charges per nm^2. In Fig. 6 *B*, the predicted reversal

potentials are indicated (*) based on a single P_{Ca}/P_{DMA} of 58 and a local negative potential that varies with ionic strength and ranges from about −7 in the 10 mM solution to −0.5 mV in the 150 mM solution.

To verify these conclusions, a more thorough set of permeability-ratio measurements was made in external mixtures of Cs^+ with Ca^{2+} or Ba^{2+} and with pure Cs^+ inside. Cs^+ was used instead of DMA^+ and both Ca^{2+} and Ba^{2+} were used over a wider concentration range to be certain that the previous conclusions did not depend on the species of permeant cations that were used. As always, reversal potentials were

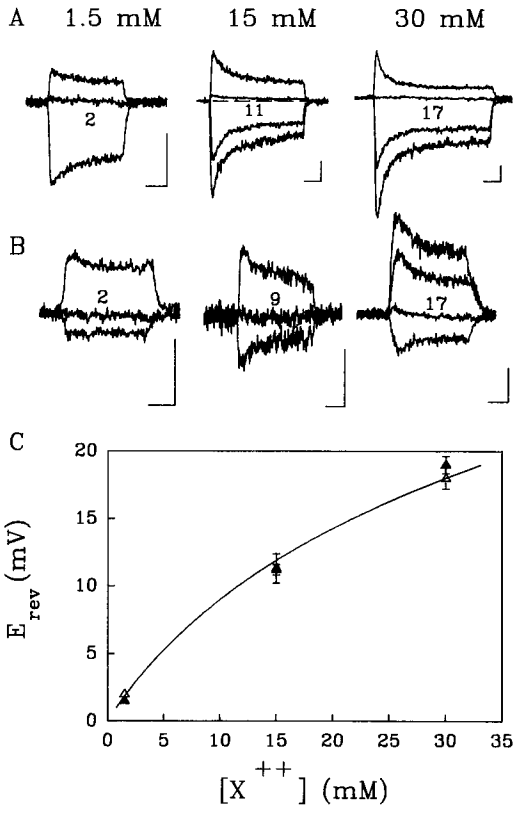

FIGURE 7. Reversal potential measurements in mixtures of 150 mM Cs^+ with different concentrations of either Ca^{2+} or Ba^{2+}. Agonist-induced, whole-cell currents are shown in symmetrical 150 mM Cs^+ with externally added 1.5, 15, and 30 mM Ca^{2+} (*A*) or Ba^{2+} (*B*). The reversal potentials are given for each set of currents. Currents are shown at the following holding potentials in Ca^{2+} (*A*): 4, 2, −4 mV in 1.5 mM; 18, 13, 5, 0 mV in 15 mM; 20, 17, 10, 0 mV in 30 mM. Currents are shown at the following holding potentials in Ba^{2+} (*B*): 4, 2, 1 mV in 1.5 mM; 14, 9, 4 mV in 15 mM; 37, 27, 17, −3 mV in 30 mM. The scale bars represent 25 pA and 1 s. Although currents were measured at other holding potentials, they are not shown to simplify the figure. The results indicate that the reversal potentials are not altered by a species specific modulation of the channel. (*C*) The reversal potentials are plotted versus the activity of the divalent cation (Ca^{2+}, △, or Ba^{2+}, ▲) added to the external 150 mM Cs^+. The theoretical line drawn through the data is based on the extended Goldman-Hodgkin-Katz equation with a constant permeability ratio (P_{++}/P_{Cs}) of 12 and no surface potential.

measured as the difference between control solutions that had no divalent cations and solutions that contained different concentrations of divalent cations. With 150 (112) mM Cs^+ inside, the reversal potentials were measured in external solutions of 150 (112, 107, 104) mM Cs^+ with 1.5 (0.36), 15 (3.3), or 30 (6.3) mM Ca^{2+} (Fig. 7 *A*) or Ba^{2+} (Fig. 7 *B*). Fig. 7 *C* shows that the permeability ratios, P_{Ca}/P_{Cs} and P_{Ba}/P_{Cs}, are concentration independent. A single permeability ratio of ~12 describes the Erev measurements over the full range of Ca^{2+} or Ba^{2+} activities that were tested. This result provides further evidence that even when considering monovalent and divalent cations the NMDA receptor behaves as a single-occupancy channel.

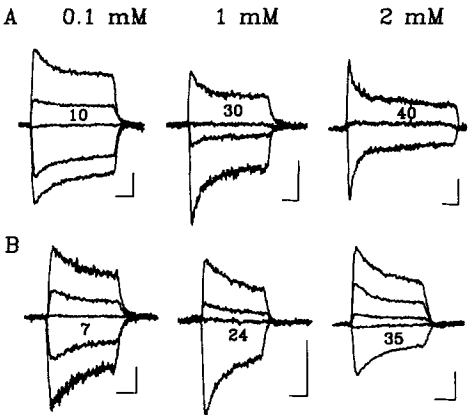

FIGURE 8. Reversal potential measurements in mixtures of 10 mM Cs^+ with different concentrations of either Ca^{2+} or Ba^{2+}. Agonist-induced, whole-cell currents are shown in symmetrical 10 mM Cs^+ with externally added 0.1, 1, and 2 mM Ca^{2+} (*A*) or Ba^{2+} (*B*). The reversal potentials are given for each set of currents. Currents are shown at the following holding potentials in Ca^{2+} (*A*): 25, 15, 10, 0, −5 mV in 0.1 mM; 35, 30, 25, 15 mV in 1 mM; 50, 40, 30 mV in 2 mM. Currents are shown at the following holding potentials in Ba^{2+} (*B*): 26, 16, 7, −19, −39 mV in 0.1 mM; 39, 29, 24, −41 mV in 1 mM; 60, 50, 40, 35, 0 mV in 2 mM. Although currents were measured at other holding potentials, they are not shown to simplify the figure. The scale bars represent 20 pA and 1 s.

Then, reversal potentials were measured again after all the solutions were diluted 15 times to obtain 10 (9.0, 8.9, 8.8) mM Cs^+ with 0.1 (0.053), 1 (0.50), or 2 (0.95) mM Ca^{2+} (Fig. 8 *A*) or Ba^{2+} (Fig. 8 *B*). Because the ratio of divalent to monovalent cations is held constant in the bulk solution, the reversal potentials would be equal in the high and low ionic strength solutions if there were no local surface potential. In Fig. 9, the reversal potentials are plotted versus the constant ratio of cations, $[X^{++}]/[Cs^+]$, showing that the positive reversal potential shifts are larger in the 10-mM solution (Fig. 9, *Low*). The data at high ionic strength are described by the simple GHK equation (Eq. 2), as shown also in Fig. 7 *C*. In the high ionic strength of 150 mM, a P_{++}/P_{Cs} equal to 12 with a negligible local surface potential was used to

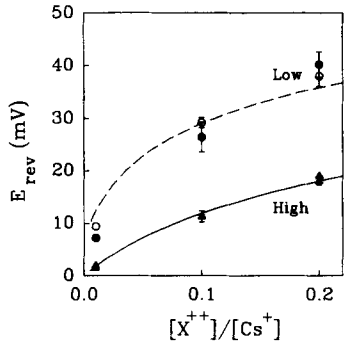

FIGURE 9. Reversal potentials in low and high ionic strength solutions having a constant ratio of monovalent to divalent cations. The reversal potentials ($n \geq 3$, SEM), as determined in Figs. 7 and 8, are plotted versus the ratio of the concentration of the divalent cation (Ca^{2+} or Ba^{2+}) to that of the concentration of Cs^+. Although the ratio of the concentrations remained constant, the concentrations changed from 150 mM Cs^+ with 1.5, 15, or 30 mM Ca^{2+} (△) or Ba^{2+} (▲; labeled *High*) to 10 mM Cs^+ with 0.1, 1, or 2 mM Ca^{2+} (○) or Ba^{2+} (●; labeled *Low*). In the high ionic strength solutions, the solid theoretical line is based on the extended Goldman-Hodgkin-Katz equation with a permeability ratio (P_{++}/P_{Cs}) of 12 and no surface potential. In the low ionic strength solutions, the dashed theoretical line is based on the same value of the permeability ratio ($P_{++}/P_{Cs} = 12$) and a small negative surface potential produced by a charge density of 0.02 per nm^2. If there were no surface potential effects, the two sets of data and the theoretical lines would lie on top of each other. Activity coefficient corrections were used in the calculations as described in the Materials and Methods.

produce the solid line. In the low ionic strength of 10 mM, the same constant permeability ratio was used but the surface potential became significant (~ -7 mV), producing the dashed line. The same value of a low charge density could describe all the results, including the single-channel conductances obtained in NH_4^+ (Figs. 3 and 4) and the permeability measurements in mixtures of DMA^+ and Ca^{2+} (Fig. 6). The conclusions of all of these experiments are in quantitative agreement that there is a low density of net negative charge influencing the NMDA receptor pore.

DISCUSSION

This research provides two pieces of information about the NMDA receptor channel. First, five different approaches indicate that the NMDA receptor behaves as a single-occupancy channel for both monovalent and divalent cations. That conclusion can be defined more completely. Only one cation at a time occupies a binding site or sites that are located directly in the permeation pathway. These binding sites are located in the narrow portion of the pore so that every cation encounters these sites during permeation, and cations cannot easily pass by each other in this region. Other binding sites are likely to exist in the water-filled pore, but those are in wider regions and not directly in the permeation pathway of every cation. Many of these widely separated sites may be occupied by counter ions. The site(s) in the narrow region of the pore, however, govern the permeation properties and are singly occupied owing to electrostatic repulsion between cations. Furthermore, elevated Cs^+ diminishes blockade of the channel by Mg^{2+}, indicating that Cs^+ is not occupying a site external to the Mg^{2+} blocking site. This result (Fig. 5) suggests that Mg^{2+} and Cs^+ are competing for the same site (or electrostatically indistinguishable sites). Second, measurements in a wide range of ionic strength solutions indicate that permeability ratios are only weakly affected by charged residues in or near the NMDA receptor channel. In physiologic solutions, the potential produced by local charges does not strongly influence ion permeation. In low ionic strength solutions, however, local net negative charges produce a meaningful negative potential that elevates the concentration of cations near the channel. The results indicate that electrolytes must either bind to or screen local charges in physiologic solutions so that the ionic environment near the pore is not dramatically different from bulk solution. The same, very low charge density was used to describe all the data. That estimate of the charge density depends on the models, but the general conclusions are not dependent on the models or equations used for the analysis. Given the limitations and approximate nature of the surface-charge approach (see McLaughlin, 1977; Dani, 1986), the theoretical description of the data is adequate for our purposes.

Impact on Previous Results

Previous studies of the NMDA receptor have suggested that permeation is affected either by multiple occupancy or by a local negative surface potential. Our results provide a more thorough interpretation of previous results. We are in complete agreement with earlier results that estimated the permeability ratio of Ca^{2+} to Na^+ or Cs^+ (P_{Ca}/P_+) to be ~ 12 (calculated using activities, Mayer and Westbrook, 1987; Iino et al., 1990). Those authors also found that P_{Ca}/P_+ is apparently larger in low ionic

strength solutions, just as we have shown under more varied conditions. That result is not due to multiple occupancy but, rather, is due to the influence of a local negative potential that is significant only in low ionic strength solutions. That interpretation is reinforced by another result. In higher ionic strength solutions (100 or 150 mM monovalent salts), the reversal potential responds to added external Ca^{2+} in a way that can be described by a single binding site without the need to invoke a surface potential or multiple occupancy (our Fig. 9; Mayer et al., 1987). Contrary to these findings, it has been suggested that a large negative surface potential in physiologic solutions may explain the parallel shift in the outward limb of current-voltage relationships caused by increasing external Ca^{2+} (Ascher and Nowak, 1988). In retrospect, we know that a large surface potential need not be invoked and that the apparently parallel current-voltage relationships arise because Ca^{2+} shifts the reversal potential. A related issue is that Ca^{2+} may alter the local surface potential by binding to the NMDA receptor at sites other than directly in the permeation pathway (Ascher and Nowak, 1988). Binding to external sites by Ca^{2+} could change the charge density that influences the ionic environment around the channel. Such a mechanism is consistent with our work and is supported by the finding that elevated Ca^{2+} decreases Zn^{2+} binding and decreases Zn^{2+} modulation of the receptor (Mayer, Vyklicky, and Westbrook, 1989).

Studies using cloned NMDA receptor subunits are consistent with our conclusion that there is no significant local surface potential influencing the ionic environment in physiologic solutions. Studies with cloned channels expressed in *Xenopus* oocytes indicate that ion permeation is controlled mainly by uncharged residues in transmembrane region M2 and not by nearby negatively charged residues (Mori, Masaki, Yamakura, and Mishina, 1992; Burnashev, Schoepfer, Monyer, Ruppersberg, Gunther, Seeburg, and Sakmann, 1992). A particular amino acid (asparagine 598) has a dominant role in controlling Ca^{2+} permeability of NMDA receptors composed of subunit NR1. This same amino acid in a homologous subunit, NR2, is predominant in determining the Mg^{2+} blockade of cloned NMDA receptors (Burnashev et al., 1992). Consistent with our results, a group of six negatively charged amino acids that flank transmembrane region M2 do not influence Mg^{2+} or MK-801 blockade of the channel in physiological solutions. Charged residues bracketing the membrane spanning region are located in a position to produce local potentials that could influence ion selectivity and permeation (see Dani, 1986). Because they do not, it is likely that the residues are at least partially screened or balanced by bound counter ions. It is also possible that the residues are either not directed into the pore or are not all expressing their charge because the pK of an amino acid is shifted by the presence of other charged amino acids.

Another issue that can be re-examined is the mechanism for the interaction between open channel blockers of the NMDA receptor (Mayer and Westbrook, 1987; Ascher and Nowak, 1988; Huettner and Bean, 1988). Much of the interaction between Mg^{2+} and the permeant ion Ca^{2+} can be explained by competition for a single site, consistent with the apparent competition between Mg^{2+} and Cs^{+} that we saw in Fig. 5. However, in low ionic strength solutions, it seems that the interaction between the large organic blocker MK-801 and Mg^{2+} is not competitive (Reynolds and Miller, 1988). They seem to be occupying two different sites that interact, which

would imply the channel can have multiple occupancy of sites in the permeation pathway. Several circumstances may underlie this finding. Because MK-801 is large, it may not reach the primary binding site for small cations. Therefore, MK-801 finds a low energy configuration external to that site. Mg^{2+}, however, reaches the primary site where it lingers while blocking the channel. Because electrostatic interactions reach especially far in very low ionic strength solutions, Mg^{2+} at its site speeds the off rate of MK-801 from its site by electrostatic repulsion. This low energy position for MK-801 may not be available to or may not be directly in the permeation pathway for small permeant ions: e.g., a small ion may occupy the position, but other permeant ions could pass by without being strongly influenced. The very large voltage-dependencies of some open channel blocks may be explained in the same manner, but we are now investigating that issue.

Conclusions about Ion Permeation in the NMDA Receptor Channel

The narrow region of the pore, where ions cannot easily pass by each other, holds one cation at a time. It may be that this narrow region is very short and, thus, provides only one main binding site, as is the case for the nicotinic acetylcholine receptor (Dani, 1989). Alternatively, electrostatic repulsion may allow only single occupancy of the multiple sites in this region.

The mechanism for the high Ca^{2+} conductance of the NMDA receptor is not the same as for the voltage-dependent Ca^{2+} channel (VDCC). The VDCC has two strongly interacting very high affinity sites for Ca^{2+}. The high affinity sites allow greater selectivity for Ca^{2+} and electrostatic repulsion between these sites speeds Ca^{2+} off its site and through the channel (Almers and McCleskey, 1984; Hess and Tsien, 1984). For the NMDA receptor, the affinity of the site is not as high. Thus, the selectivity is not as great, but high conductance does not require electrostatic repulsion arising from multiple occupancy to speed the ion off of its site.

In physiologic solutions, the ionic environment near the pore is not strongly influenced by a local negative potential. In low ionic strength solutions, the influence of local charges becomes important. Although we might anticipate that local charges within the channel influence the permeation process in some way, those charges do not alter the general ionic environment near the pore under normal conditions.

We thank Drs. Craig Jahr, Robin Lester, Marc Rogers, and Ms. Martha Skender for reading and commenting on the manuscript. We thank Dr. Ramon Latorre for helpful discussions about the single-channel measurements with Mg^{2+} present. The work was supported by the Whitaker Foundation and by NIH grant NS 21229.

Original version received 26 March 1993 and accepted version received 27 August 1993.

REFERENCES

Almers, W., and E. W. McCleskey. 1984. Non-selective conductance in calcium channels of frog muscle: calcium selectivity in a single-file pore. *Journal of Physiology.* 353:585–608.

Amador, M., and J. A. Dani. 1991*a*. Protein kinase inhibitor, H-7, directly affects *N*-methyl-D-aspartate receptor channels. *Neuroscience Letters.* 124:251–255.

Amador, M., and J. A. Dani. 1991*b*. MK-801 inhibition of nicotinic acetylcholine receptor channels. *Synapse.* 7:207–215.

Ascher, P., and L. Nowak. 1988. The role of divalent cations in the *N*-methyl-D-aspartate responses of mouse central neurones in culture. *Journal of Physiology.* 399:247–266.

Bliss, T. V. P., and G. L. Collingridge. 1993. A synaptic model of memory: long-term potentiation in the hippocampus. *Nature.* 361:31–39.

Burnashev, N., R. Schoepfer, H. Monyer, J. P. Ruppersberg, W. Gunther, P. H. Seeburg, and B. Sakmann. 1992. Control by asparagine residues of calcium permeability and magnesium blockade in the NMDA receptor. *Science.* 257:1415–1419.

Butler, J. N. 1968. The thermodynamic activity of calcium ion in sodium chloride-calcium chloride electrolytes. *Biophysical Journal.* 8:1426–1433.

Cecchi, X., D. Wolff, O. Alvarez, and R. Latorre. 1987. Mechanisms of Cs^+ blockade in a Ca^{2+}-activated K^+ channel from smooth muscle. *Biophysical Journal.* 52:707–716.

Dani, J. A. 1986. Ion-channel entrances influence permeation: net charge, size, shape, and binding considerations. *Biophysical Journal.* 49:607–618.

Dani, J. A. 1989. Open channel structure and ion binding sites of the nicotinic acetylcholine receptor channel. *Journal of Neuroscience.* 9:884–892.

Dani, J. A., and G. Eisenman. 1987. Monovalent and divalent cation permeation in acetylcholine receptor channels: ion transport related to structure. *Journal of General Physiology.* 89:959–983.

Grahame, D. C. 1947. The electrical double layer and the theory of electrocapillarity. *Chemical Reviews.* 41:441–501.

Green, W. N., and O. S. Andersen. 1991. Surface charges and ion channel function. *Annual Review of Physiology.* 53:341–359.

Hamill, O. P., A. Marty, E. Neher, B. Sakmann, and F. J. Sigworth. 1981. Improved patch-clamp techniques for high-resolution current recording from cells and cell-free membrane patches. *Pflugers Archiv.* 391:85–100.

Hess, P., and R. W. Tsien. 1984. Mechanism of ion permeation through calcium channels. *Nature.* 309:453–456.

Huettner, J. E., and R. W. Baughman. 1986. Primary culture of identified neurons from the visual cortex of postnatal rats. *Journal of Neuroscience.* 6:3044–3060.

Huettner, J. E., and B. P. Bean. 1988. Block of *N*-methyl-D-aspartate-activated current by the anticonvulsant MK-801: selective binding to open channels. *Proceedings of the National Academy of Sciences, USA.* 85:1307–1311.

Iino, M., S. Ozawa, and K. Tsuzuki. 1990. Permeation of calcium through excitatory amino acid receptor channels in cultured rat hippocampal neurones. *Journal of Physiology.* 424:151–165.

Jahr, C. E., and C. F. Stevens. 1987. Glutamate activates multiple single channel conductances in hippocampal neurons. *Nature.* 325:522–525.

Jahr, C. E., and C. F. Stevens. 1990. A quantitative description of NMDA receptor-channel kinetic behavior. *Journal of Neuroscience.* 10:1830–1837.

Johnson, J. W., and P. Ascher. 1990. Voltage-dependent block by intracellular Mg^{++} of *N*-methyl-D-aspartate-activated channels. *Biophysical Journal.* 57:1085–1090.

Levitt, D. G. 1986. Interpretation of biological ion channel flux data: reaction-rate versus continuum theory. *Annual Reviews of Biophysics and Biophysical Chemistry.* 15:29–57.

Lewis, C. A. 1979. Ion-concentration dependence of the reversal potential and the single channel conductance of ion channels at the frog neuromuscular junction. *Journal of Physiology.* 286:417–445.

Lewis, C. A., and C. F. Stevens. 1979. Mechanism of ion permeation through channels in a postsynaptic membrane. *In* Membrane Transport Processes. C. F. Stevens and R. W. Tsien, editors. Raven Press, NY. 133–151.

Mayer, M. L., and G. L. Westbrook. 1987. Permeation and block of *N*-methyl-D-aspartic acid receptor channels by divalent cations in mouse cultured central neurones. *Journal of Physiology.* 394:501–527.

Mayer, M. L., G. L. Westbrook, and P. B. Guthrie. 1984. Voltage-dependent block by Mg^{++} of NMDA responses in spinal cord neurones. *Nature.* 309:261–263.

Mayer, M. L., L. Vyklicky, Jr., and G. L. Westbrook. 1989. Modulation of excitatory amino acid receptors by group IIB metal cations in cultured mouse hippocampal neurones. *Journal of Physiology.* 415:329–350.

Mayer, M. L., G. L. Westbrook, and L. Vyklicky, Jr. 1988. Sites of antagonist action on *N*-methyl-D-aspartic acid receptors studied using fluctuation analysis and a rapid perfusion technique. *Journal of Neurophysiology.* 60:645–663.

MacDermott, A. B., M. L. Mayer, G. L. Westbrook, S. J. Smith, and J. L. Barker. 1986. NMDA-receptor activation increases cytoplasmic calcium concentration in cultured spinal cord neurones. *Nature.* 321:519–522.

McLaughlin, S. 1977. Electrostatic potentials at membrane-solution interfaces. *In* Current Topics in Membrane and Transport. F. Bronner and A. Kleingellen, editors. Academic Press, NY. 71–145.

Mori, H., H. Masaki, T. Yamakura, and M. Mishina. 1992. Identification by mutagenesis of a Mg^{++}-block site of the NMDA receptor channel. *Nature.* 358:673–675.

Neher, E. 1975. Ionic specificity of the gramicidin channel and the thallous ion. *Biochimica et Biophysica Acta.* 401:540–544.

Neyton, J., and C. Miller. 1988. Potassium blocks barium permeation through the high-conductance Ca^{2+}-activated K^+ channel. *Journal of General Physiology.* 92:549–567.

Nowak, L., P. Bregestovski, P. Ascher, A. Herbet, and A. Prochiantz. 1984. Magnesium gates glutamate-activate channels in mouse central neurones. *Nature.* 307:462–465.

Reynolds, I. J., and R. J. Miller. 1988. Multiple sites for the regulation of the NMDA receptor. *Molecular Pharmacology.* 33:581–584.

Vernino, S., M. Amador, C. W. Luetje, J. Patrick, and J. A. Dani. 1992. Calcium modulation and high calcium permeability of neuronal nicotinic acetylcholine receptors. *Neuron.* 8:127–134.

Zarei, M. M., and J. A. Dani. 1992. Calcium permeability of the NMDA receptor is influenced by negative charges in or near the channel. *Biophysical Journal.* 61:104*a*. (Abstr).